Astronomy
&
Astrophysics

The SOPHIE search for northern extrasolar planets[*]

VIII. Follow-up of ELODIE candidates: long-period brown-dwarf companions[**]

F. Bouchy[1,2], D. Ségransan[2], R. F. Díaz[1,2], T. Forveille[3], I. Boisse[1,4], L. Arnold[5], N. Astudillo-Defru[3], J.-L. Beuzit[3],
X. Bonfils[3], S. Borgniet[3], V. Bourrier[2,6], B. Courcol[1], X. Delfosse[3], O. Demangeon[1], P. Delorme[3], D. Ehrenreich[2],
G. Hébrard[5,6], A.-M. Lagrange[3], M. Mayor[2], G. Montagnier[5,6], C. Moutou[1,7], D. Naef[2], F. Pepe[2], C. Perrier[3],
D. Queloz[2], J. Rey[2], J. Sahlmann[8], A. Santerne[4], N. C. Santos[4,9], J.-P. Sivan[1], S. Udry[2], and P. A. Wilson[6]

1   Aix-Marseille Université, CNRS, Laboratoire d'Astrophysique de Marseille UMR 7326, 13388 Marseille Cedex 13, France
2   Observatoire de Genève, Université de Genève, 51 Ch. des Maillettes, 1290 Sauverny, Switzerland
3   Université Grenoble Alpes, CNRS, IPAG, 38000 Grenoble, France
4   Instituto de Astrofísica e Ciências do Espaço, Universidade do Porto, CAUP, 4150-762 Porto, Portugal
5   Aix-Marseille Université, CNRS, Observatoire de Haute-Provence, Institut Pythéas, 04870 St Michel l'Observatoire, France
6   Institut d'Astrophysique de Paris, UMR 7095 CNRS, Université Pierre & Marie Curie, 98bis Bd Arago, 75014 Paris, France
7   Canada France Hawaii Telescope Corporation, Kamuela, HI 96743, USA
8   European Space Agency, European Space Astronomy Centre, PO Box 78, Villanueva de la Canada, 28691 Madrid, Spain
9   Departamento de Física e Astronomia, Faculdade de Ciências, Universidade do Porto, 4150-762 Porto, Portugal

ABSTRACT

Long-period brown dwarf companions detected in radial velocity surveys are important targets for direct imaging and astrometry to calibrate the mass–luminosity relation of substellar objects. Through a 20-yr radial velocity monitoring of solar-type stars that began with ELODIE and was extended with SOPHIE spectrographs, giant exoplanets and brown dwarfs with orbital periods longer than ten years are discovered. We report the detection of five new potential brown dwarfs with minimum masses between 32 and 83 $M_{\rm Jup}$ orbiting solar-type stars with periods longer than ten years. An upper mass limit of these companions is provided using astrometric Hipparcos data, high-angular resolution imaging made with PUEO, and a deep analysis of the cross-correlation function of the main stellar spectra to search for blend effects or faint secondary components. These objects double the number of known brown dwarf companions with orbital periods longer than ten years and reinforce the conclusion that the occurrence of such objects increases with orbital separation. With a projected separation larger than 100 mas, all these brown dwarf candidates are appropriate targets for high-contrast and high angular resolution imaging.

Key words. techniques: radial velocities – binaries: spectroscopic – stars: low-mass – brown dwarfs – stars: general

1. Introduction

Brown dwarfs (BD) are substellar objects in the mass range of approximately 13–80 Jupiter masses; they have enough mass to burn deuterium, but are too light to permit hydrogen burning in their inner cores (Burrows et al. 1997; Chabrier & Baraffe 2000; Spiegel et al. 2011). BDs constitute intermediate objects between giant planets and low-mass stars, but there is not a complete consensus about their formation mechanisms. The separation between planet and brown dwarf population may not only be related to the mass, but also to the formation scenario. Core-accretion models predict the formation of objects as heavy as 25 $M_{\rm Jup}$ (Mordasini et al. 2009). BD companions orbiting solar-type stars with periods of up to about ten years clearly occur less frequently (≤1%) than planetary systems and stellar binaries

(e.g., Grether & Lineweaver 2006; Sahlmann et al. 2011; Ma & Ge 2014). Statistical properties of BD companions, such as frequency, separation, eccentricity, and mass ratio distribution, as well as the relation of these properties to their host stars, should permit us to distinguish between different formation and evolution models.

Most of the brown dwarf companions have been discovered in radial velocity (RV) surveys (e.g., Nidever et al. 2002; Sahlmann et al. 2011; Díaz et al. 2012). In these programs, which were designed to find exoplanets, brown dwarfs are easily detected by their strong RV signatures. However, radial velocity measurements alone do not constrain the orbit inclination and therefore provide only the minimum mass. When available, complementary observational constraints, such as the astrometric motion of the host star, a deep analysis of the spectra to search for a blend or a secondary component, or a photometric transit, are required to attempt determining the true mass or at least to firmly exclude the stellar nature of the companion.

So far, only a few brown-dwarfs have been detected in radial velocity with orbital periods longer than ten years; this is a somewhat biased result because there have been relatively few

---

Table 1. Target characteristics and summary of observations.

Target Name	RA [deg]	Dec [deg]	V	$B-V$	Spectral type	$v \sin i$ [km s^{-1}]	Distance [pc]	Time span [yr]	Nmeas Elodie/Sophie
HD 10844	26.687	25.918	8.13	0.63	F8V	1.9 ± 1	52.3	12.78	25/27
HD 14348	34.971	31.337	7.19	0.60	F5V	5.4 ± 1	56.6	16.85	61/38
HD 18757	46.040	61.706	6.64	0.63	G4V	1.4 ± 1	24.2	16.75	31/43
HD 72946	128.964	6.623	7.25	0.71	G5V	3.9 ± 1	26.2	16.04	45/23
HD 209262	330.476	4.770	8.00	0.69	G5V	3.0 ± 1	49.7	12.70	15/21

long-term surveys. These objects are important targets for direct imaging and astrometry with the aim to calibrate the mass–luminosity relation of substellar objects. Since the end of 2006, the SOPHIE consortium conducts a large program to search for exoplanets (Bouchy et al. 2009). One of the different subprograms focuses on following-up the drifts and long-period signals detected within the ELODIE historical program initiated on the 1.93 m telescope at the Observatoire de Haute-Provence (OHP) by M. Mayor and D. Queloz in 1994. This program has monitored about 400 solar-type stars (from F5 to K0 dwarfs) in 12 yr and led to the detection of 24 exoplanets (e.g., Mayor & Queloz 1995; Perrier et al. 2003; Naef et al. 2004). In the past years, this program was focused on monitoring RV drifts that were identified as incomplete orbits of gravitationally bound companions. Since 2007, we have continued this program with the SOPHIE spectrograph with the objective to characterize orbital parameters of exoplanets similar to Jupiter and Saturn in our solar system and brown dwarfs with orbital periods longer than eight to ten years. About 50 targets with a slow RV drift were selected from the original ELODIE sample and are followed-up with SOPHIE. This unique sample allows extending the time base to more than 20 years to find substellar companions beyond 5 AU. As part of this subprogram, we reported the detection of two Jupiter-analogs around HD 150706 and HD 222155, we refined the parameters of the long-period planets HD 154345b and HD 89307b, and we determined the first reliable orbit for HD 24040b (Boisse et al. 2012).

In this paper, we report the detection of five new brown dwarf candidates with minimum masses of between 32 and 78 M_{Jup} orbiting solar-type stars with period longer than ten years. We attempt to derive an upper limit on the true mass of these companions to determine their nature using astrometric HIPPARCOS data, high-angular resolution imaging made with PUEO for two of our targets, and deep analysis of the cross-correlation function (CCF) of our spectra to search for a blend effect or a faint secondary component. Such a CCF analysis was performed on HD 16702 and allowed identifying the secondary component. We also present in the Appendix an update of the orbital parameter of the low-mass star HD 29461b that was recently published by Griffin (2012) as well as the long-term RV drift of HD 175225, which is induced by a low-mass stellar companion.

2. Spectroscopic observations

The targets reported in this paper and their basic stellar characteristics are listed in Table 1. The parallaxes are derived from the new HIPPARCOS reduction (van Leeuwen 2007). The stellar rotation parameter $v \sin i$ is derived from the calibration of the SOPHIE cross-correlation function by Boisse et al. (2010) with an uncertainty of ~1 km s^{-1}. The time span of the observations and the numbers of the ELODIE and SOPHIE measurements are listed in Table 1.

Spectroscopic observations of our targets were first conducted with the ELODIE spectrograph (Baranne et al. 1996)

mounted on the 1.93 m telescope at OHP between late 1993 and mid-2006. The stars were then monitored by the SOPHIE spectrograph (Perruchot et al. 2008) from early 2007 to late 2014. The spectrograph configuration, the observing mode, and the data reduction were the same as those described in Boisse et al. (2012).

One of the main SOPHIE systematic effects was caused by the insufficient scrambling of the fiber link and the high sensitivity of the spectrograph to illumination variation. Seeing change at the fiber input introduced radial velocity changes. This so-called seeing effect on SOPHIE has been described by Boisse et al. (2010, 2011), Díaz et al. (2012), and Bouchy et al. (2013). Considering that variations in the pupil illumination produce a differential RV effect along spectral orders, the difference between RVs measured in each half of the spectral orders can be used to partially correct the main RV. We systematically applied the correction of the seeing effect by computing the RV difference between the left part (or blue side) and right part (or red side) of the spectral orders and using the average correlation coefficient of −1.04 estimated on standard stars (Bouchy et al. 2013). We added quadratically a systematic RV error of 6 m s^{-1} on the SOPHIE measurements corresponding to the average RV RMS measured on these stars. In June 2011 (BJD = 2 455 730), a piece of octagonal-section fiber was implemented in the SOPHIE fiber link and significantly improved the radial velocity precision by eliminating the seeing effect, see Bouchy et al. (2013). We checked on standard stars that the RV offset introduced by the instrumental upgrade is smaller than the systematic errors of SOPHIE. Since this change and despite a clear improvement in RV precision on times scales of a few tens of days, some intervention within the instrument and strong variations of the outside temperature propagated to the tripod of the spectrograph introduced zero-point offsets. The systematic drift was corrected using a set of RV constant star and following the approach described by Courcol et al. (2015).

3. Data analysis

3.1. Stellar characteristics

Spectra obtained without simultaneous thorium-argon calibration and with signal-to-noise ratios in the range of 150–200 were used to accurately derive the stellar effective temperature T_{eff}, surface gravity $\log g$, and metallicity [Fe/H]. The spectroscopic analysis method is described in Santos et al. (2004) and Sousa et al. (2008). In brief, the procedure is based on the equivalent widths of the FeI and FeII lines and the iron excitation and ionization equilibrium, which is assumed to be in local thermodynamic equilibrium. Using the derived spectroscopic parameters as input, stellar masses $M_\star$ were derived from the calibration of Torres et al. (2010) with a correction following Santos et al. (2013). Errors were computed from 10 000 random values of the stellar parameters within their error bars and assuming a

Table 2. Stellar parameters.

Target name	$T_{\rm eff}$ [K]	$\log g$ [cgs]	[Fe/H] [dex]	$v$micro [km s^{-1}]	$M_\star$ [$M_\odot$]	Age [Gyr]	$\log R'_{\rm HK}$
HD 10844	5845 ± 37	4.43 ± 0.05	-0.06 ± 0.03	1.08 ± 0.05	0.98 ± 0.07	6.7 ± 1.5	-4.85 ± 0.05
HD 14348	6237 ± 47	4.51 ± 0.07	0.28 ± 0.03	1.53 ± 0.06	1.20 ± 0.08	2.2 ± 0.3	-4.95 ± 0.05
HD 18757	5656 ± 28	4.41 ± 0.04	-0.27 ± 0.02	0.84 ± 0.04	0.88 ± 0.06	11.4 ± 0.1	-4.94 ± 0.05
HD 72946	5686 ± 40	4.50 ± 0.06	0.11 ± 0.03	0.83 ± 0.06	0.96 ± 0.07	2.0 ± 1.7	-4.74 ± 0.05
HD 209262	5815 ± 28	4.41 ± 0.04	0.10 ± 0.02	1.14 ± 0.03	1.02 ± 0.07	4.7 ± 1.8	-4.97 ± 0.05

Gaussian distribution. Ages were estimated using the method[1] described by da Silva et al. (2006) using PARSEC stellar tracks and isochrones from Bressan et al. (2012). The stellar activity level was estimated from the emission in the core of the Ca II H and K-bands measured on each SOPHIE spectra with the calibration described in Boisse et al. (2010). The average values derived from this analysis are reported in Table 2 with an estimated uncertainty of 0.05.

3.2. Radial velocity analysis and orbital solutions

ELODIE and SOPHIE radial velocities were fit using the Bayesian genetic software *Yorbit*, which is briefly described in Ségransan et al. (2011). The main advantage of a genetic algorithm compared to other advanced methods such as a Markov chain Monte Carlo method (hereafter MCMC) with parallel tempering is that it allows probing the full model parameter space in an extremely efficient way. The first step of the radial velocity data analysis consists of identifying significant periodic signals in the data. This is done using the General Lomb-Scargle periodogram algorithm (Zechmeister & Kürster 2009), which is applied to the radial velocity measurements. False-alarm probabilities are estimated through a bootstrap approach by permuting the data. When a significant peak is located at a given period, the corresponding Keplerian is adjusted. For multiple Keplerians, the adjusted component is removed, the process is repeated several times until no significant peak remains, and all parameters are readjusted at each step of the analysis. However, the population at the end of the evolution is not statistically reliable owing the intrinsic nature of genetic algorithm, which is based on genome crossover and mutation. To obtain robust confidence intervals for the Keplerian parameters as well as an estimate of the additional noise present in the data (called nuisance parameter), we further probed the parameter space with an MCMC algorithm with a Metropolis-Hastings algorithm. This is based on the formalism described in Collier Cameron et al. (2007) with several thousand chains drawn from the final genetic algorithm population. Each chain runs several thousand times to retrieve a statistically reliable population. For poorly constrained planetary systems, the Bayesian formalism described in Gregory (2007) is used. Our MCMC probes the following set of parameters: $\log P$, $\sqrt{e}\cos\omega$, $\sqrt{e}\sin\omega$, $\log K$, epoch of periastron $T_{\rm p}$ or epoch of minimum RV $T_{\rm RVmin}$, global RV offset $(V_0 + Ke\cos\omega)$ using SOPHIE as reference, and the RV offset between ELODIE and SOPHIE (ΔV_{ES}). The noise model follows a simple normal law with a standard deviation derived from the observation errors and a nuisance parameter $(\sigma_{\rm tot}^2 = \sigma^2 + s^2)$. Jeffrey priors are used for the period, the radial velocity semi-amplitude, and the nuisance parameter, while uniform priors are used for the other parameters.

The RV offset between the two instruments was described and calibrated by Boisse et al. (2012). It is a function of the

---
[1] http://stev.oapd.inaf.it/param

Table 3. Parameters of the HIPPARCOS astrometric observations.

Target name	HIP	Nmeas	Time span [days]	σ [mas]
HD 10844	8285	94	1069	3.34
HD 14348	10868	82	1096	1.69
HD 18757	14286	129	1043	2.59
HD 72946	42173	61	759	1.71
HD 209262	108761	57	1084	3.23

$B - V$ index and the cross-correlation mask used. However, considering the quite large uncertainty of the RV offset relation (23 m s^{-1} rms), we decided to let this parameter free to vary for the Keplerian fit. For all the candidates we also tested a model including a long-term drift in addition to the Keplerian, but no significant drift was found, or it was strongly correlated to the ELODIE-SOPHIE offset. No significant additional signals were found on the RV residuals for the five targets. The orbital solutions are listed in Table 4, and each candidate is discussed in Sect. 4.

3.3. Diagnostic for resolving the nature of the companions

The RV analysis provides a minimum mass for the companion within the range of brown dwarf masses. We used other diagnostics to attempt to derive an upper limit on the mass. More specifically, we used HIPPARCOS astrometry, high angular resolution imaging, and bisector span and CCF diagnostics.

3.3.1. HIPPARCOS astrometry

For the five BD candidates, we used the new HIPPARCOS reduction (van Leeuwen 2007) to search for signatures of orbital motion in the Intermediate Astrometric Data (IAD). The analysis was performed as described in Sahlmann et al. (2011) using the orbital elements given by the RV analysis and reported in Table 4. The basic parameters of the HIPPARCOS observations relevant for the astrometric analysis are listed in Table 3.

For the five BD candidates we found no detectable signal of a corresponding astrometric motion in the HIPPARCOS data. The main reason is that the orbital periods are very long and the astrometry data cover only 3−23% of the orbital phase. This inhibits a significant detection even though the expected minimum signals are quite strong (4−24 mas) compared to the measurement precision. Furthermore, it cannot be excluded that most of the strong general signal is absorbed into a slightly incorrect proper motion.

3.3.2. Bisector span analysis

Following the approach described by Díaz et al. (2012), we examined the bisector span of the SOPHIE CCF of our BD candidates to check whether significant variation and a correlation with RV measurements can reveal a relatively luminous

**Table 4.** Median and 1-σ limit of posterior parameters derived from our MCMC analysis.

Parameters	HD 10844	HD 14348	HD 18757	HD 72946	HD 209262
P [yr]	$31.6^{+2.7}_{-2.1}$	$12.987^{+0.017}_{-0.013}$	109^{+18}_{-16}	$15.93^{+0.15}_{-0.13}$	$14.88^{+0.37}_{-0.26}$
K [m s^{-1}]	873^{+54}_{-35}	$575.0^{+2.2}_{-2.6}$	$665.8^{+5.9}_{-5.3}$	776 ± 9.0	385^{+13}_{-11}
e	$0.568^{+0.022}_{-0.020}$	0.455 ± 0.004	0.943 ± 0.007	0.495 ± 0.006	$0.347^{+0.010}_{-0.008}$
ω [deg]	-94.9 ± 1.4	$65.12^{+0.55}_{-0.64}$	$44.0^{+0.5}_{-0.4}$	71.0 ± 1.6	$-104.1^{+3.1}_{-3.5}$
$T_\mathrm{p} - 2\,450\,000$	3876.7 ± 16	5265.6 ± 4.5	5220.0 ± 0.8	5958 ± 10	6766 ± 6
V_0 [km s^{-1}]	$-42.708^{+0.035}_{-0.054}$	$-4.231^{+2.2}_{-2.6}$	$-2.201^{+0.006}_{-0.005}$	29.527 ± 0.008	$-43.329^{+0.013}_{-0.012}$
ΔV_{ES} [km s^{-1}]	-98^{+104}_{-70}	-57 ± 3.7	$-120^{+9.5}_{-8.0}$	-113 ± 14	-165 ± 24
Jitter s (E/S) [m s^{-1}]	17.8/1.2	14.8/5.3	1.4/2.7	21.8/15.5	14.3/3.3
a [AU]	$10.18^{+0.62}_{-0.49}$	5.95 ± 0.10	$22.2^{+2.5}_{-2.3}$	6.37 ± 0.11	$6.16^{+0.15}_{-0.13}$
a [mas]	195^{+12}_{-9}	105.1 ± 1.7	917^{+103}_{-95}	243.1 ± 4.2	$123.9^{+3.0}_{-2.6}$
Mc sin $i[M_\mathrm{Jup}]$	$83.4^{+6.4}_{-5.0}$	48.9 ± 1.6	35.2 ± 1.2	60.4 ± 2.2	$32.3^{+1.6}_{-1.5}$
Mc, upper-lim [$M_\odot$]	0.4	0.35	0.13	0.2	0.4

companion polluting the peak of the primary star. The detection of a correlation indicates that the velocity signal is the result – at least in part – of a deformation of the stellar CCF. For the five targets the bisector span varies only negligibly and does not exhibit any significant correlation with radial velocity measurements; this excludes massive M dwarfs. The correlation slopes were systematically smaller than 8 m s^{-1} per km s^{-1} within the uncertainties. However, such a non-detection does not definitively exclude low-mass stellar companions. Simulations indicate that only massive M dwarfs heavier than 0.5 $M_\odot$ can be firmly excluded.

3.3.3. Search for a second component in the CCF

If the companion is relatively bright, we expect that it is blended within the main spectrum and then pollutes the CCF of the primary star. To search for a secondary peak in our SOPHIE CCFs, we proceeded in the follow way: first we built the CCFs using an M mask to maximize the contribution of a suspected low-mass star companion. Then we shifted all the CCFs to the systemic velocity V_0 and averaged them, after normalization of the minimum and maximum of the CCF, to build a master CCF. We then subtracted this master CCF from all the individual CCFs shifted to the systemic velocity. The velocity of the second component Vc is expected to be at $-V_1/q$ with respect to the systemic velocity V_0, with V_1 the velocity of the main component and q the mass ratio $Mc/M_\star$. Considering that all individual CCFs are shifted to the systemic velocity, this second component is expected to be at $(V_0 - V_1) \times (1 + 1/q)$. To increase the detection capability, we combined all the CCF residuals after shifting them to this last quantity with q varying from 0.1 to 0.6. For each value of q we computed the dispersion of the average of CCF residuals and searched for a significant peak centered at the systemic velocity.

We tested our approach on HD 16702, which was first identified by Díaz et al. (2012) to have a companion with a minimum mass of 48.7 M_Jup. These authors showed that HIPPARCOS astrometric analysis and CCF simulations lead to a companion mass of 0.55 $\pm$ 0.14 $M_\odot$ and 0.40 $\pm$ 0.05 $M_\odot$, respectively. In the average CCF residuals, shown in Fig. 1, we find a deepest secondary peak of 1.3 $\pm$ 0.1% when a shift of $(3.5 \pm 0.4) \times (V_0 - V_1)$ is imposed, hence for a mass ratio $q = 0.4 \pm 0.06$. The uncertainty on the shift applied to have the deepest second peak was estimated considering the noise level within the continuum (0.1%)
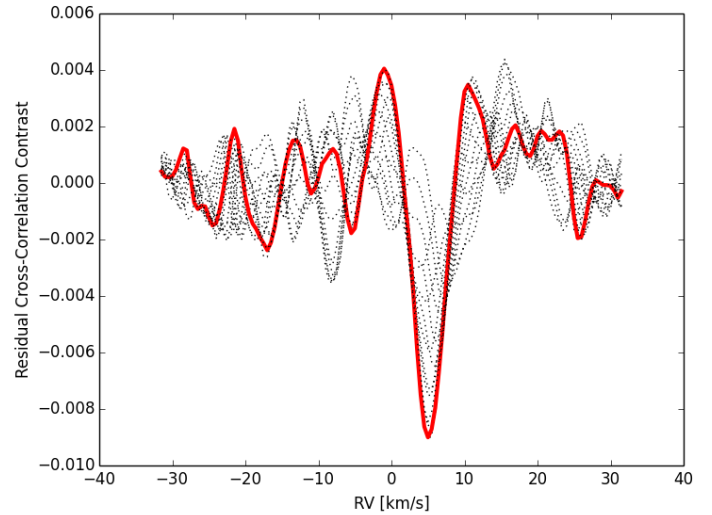
Fig. 1. Averaged CCF residuals of HD 16702 for different radial velocity shifts. The deepest peak (red curve) occurs for a shift corresponding to a mass ratio of 0.4.

and determining the shift limit, which produced a peak depth of 1.2%.

Given a primary mass of 0.98 $M_\odot$, the companion is then an M2-type star of 0.39 $\pm$ 0.06 $M_\odot$ in agreement with Díaz et al. (2012). This value also agrees with the identification of a second component in the spectra by Kolbl et al. (2015) with an estimated T_eff of 3500 $\pm$ 250 K and contributing to 1.06% of the total flux. More recently, Santerne et al. (2015) performed blend models with PASTIS (Díaz et al. 2014) and derived a companion mass of 0.35 $\pm$ 0.03 $M_\odot$.

We estimated that for HD 16702 the detection limit is close to 0.3%. However, this approach requires several observations well spread across the orbit, and the systemic velocity should be known to correctly stack and average the CCFs. Furthermore, the effectiveness of the approach strongly depends on the orbital parameters, the number of measurements, and the phase coverage.

We applied this search for a second component on our candidates, but without any significant detection. To estimate the effectiveness of the approach and derive an upper limit, we injected an artificial second component into the CCFs that corresponds to a companion with a velocity at $Vc + (Vc - V_1)/q$, a CCF contrast from 0.2 to 2% of the primary, and the same CCF

FWHM as the primary. We note that a larger CCF FWHM of the secondary, although not expected for low-mass stars of several billion years, reduces the detection sensitivity. The detection limit obtained a range from 0.5% up to 2% for the worst cases like HD 10844 and HD 209262, for which the SOPHIE velocities only cover one side with respect to the systemic velocity. In this case the second component is not well averaged and not enough diluted when computing the master CCF. It was therefore partially removed in all the individual CCFs when we subtracted the master CCF. Assuming that the CCF contrast ratio could be used as a rough estimate of the flux ratio between primary and secondary, we derive an upper mass limit using the evolutionary models for the main sequence of low-mass stars by Baraffe et al. (2015) taking into account the mass and age of the primary. The derived upper limits are in the range of 0.18–0.4 $M_\odot$ and are reported in Table 4. The lowest upper limit of 0.18 $M_\odot$ is found for HD 18757.

3.3.4. High-resolution imaging with PUEO

HD 14348 and HD 18757 were observed as filler targets during a program dedicated to mass measurements for M dwarfs at the 3.6 m Canada-France-Hawaii Telescope (CFHT) using PUEO, the CFHT Adaptive Optics Bonnette (Rigaut et al. 1998), and the KIR infrared camera (Doyon et al. 1998). The observing procedure is described by Delfosse et al. (1999). High angular resolution imaging for these two stars was analyzed to derive a detection limit for the companion. The flux detection limit was converted into an upper mass limit considering the age of the primary and using the models NEXTGEN for low-mass stars (Baraffe et al. 1998) and DUSTY for brown dwarfs (Allard et al. 2001). The RV orbital parameters and the mass of the primary were used to compute the sky-projected orbital separation of the companion relative to the host star at the date of PUEO observations assuming different orbital inclinations.
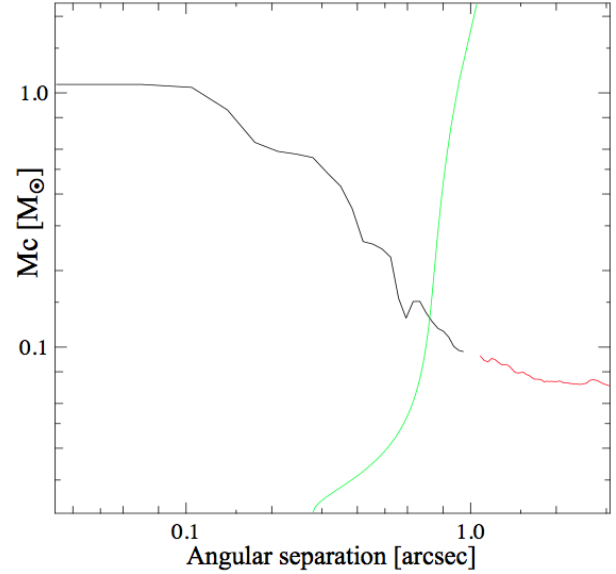
Figure 2 shows the mass detection limit as function of the angular separation for HD 18757. The green line represents the projected separation varying the orbital inclination. Companions along the green line and above black line (NEXTGEN) or red line (DUSTY) are excluded. This gives an upper limit of 0.13 $M_\odot$ for HD 18757b, which is lower than the upper limit derived from the CCF analysis.

For HD 14348, the upper limit is 0.6 $M_\odot$, which is well above the upper limit derived from the CCF analysis because the angular separation is close to 0.1 arcsec, just below the diffraction limit of the CFHT in K-band (0.12 arcsec).

4. Long-period brown dwarf companions

4.1. HD 10844

HD 10844 is a V = 8.13 mag F8V star with a mass $M_\star$ of 0.98 $M_\odot$ located at 52.3 parsec from the Sun. The Keplerian fit to the RV measurements, listed in Table 5, indicates a companion of minimum mass $Mc \sin i$ = 83.4 M_{Jup} on a 30-yr orbit, with an eccentricity e = 0.57. With such a minimum mass, HD 10844b is fairly likely to be stellar, since the inclination only needs to be slightly less than edge-on. Although the measurement time-span covers less than half of the orbital period of HD 10844, the Keplerian fit is quite well constrained becrause the orbit is eccentric and has a large semi-amplitude. The instrumental offset between ELODIE and SOPHIE is adjusted to $-98\,^{+104}_{-70}$ m s^{-1} in agreement with the expected one at -66 ± 23 m s^{-1}. Using the expected instrumental offset as prior

Fig. 2. Mass detection limit as function of angular separation for HD 18757 observed with PUEO. The black and red curves correspond to NEXTGEN and DUSTY models, respectively. The green line represents the projected separation varying the orbital inclination and shows that no companion with a mass higher than 0.13 $M_\odot$ was detected.
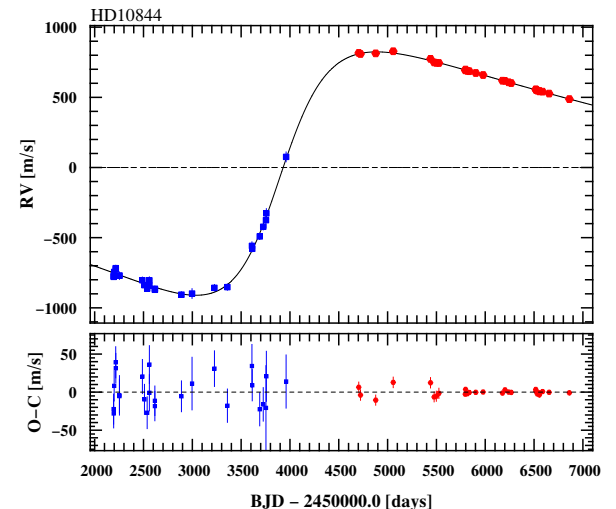
Fig. 3. Radial velocity curve of HD 10844 obtained with ELODIE (blue) and SOPHIE (red).

does not significantly change the result, but it reduces the uncertainties with $P = 32.3^{+1.0}_{-1.2}$ yr and $K = 885^{+12}_{-11}$ m s^{-1}. Systematic errors of 17.8 m s^{-1} and 1.2 m s^{-1} were quadratically added to ELODIE and SOPHIE, respectively, to obtain the reduced $\chi^2 = 1$.

4.2. HD 14348

HD 14348 is a F5V star with V = 7.2 mag located at 56.6 parsec from the Sun, with a mass of 1.2 $M_\odot$. The RV measurements listed in Table 6 show a peak-to-peak variation of 1150 m s^{-1} that reveal the presence of an $Mc \sin i$ = 48.9 M_{Jup} companion on a 13-yr orbit, with an eccentricity of 0.45. The instrumental offset between ELODIE and SOPHIE is adjusted to -57 ± 3.7 m s^{-1}, which agrees with the expected offset at -53 ± 23 m s^{-1}. Systematic errors of 14.8 m s^{-1} and 5.3 m s^{-1} were quadratically added to ELODIE and SOPHIE, respectively.
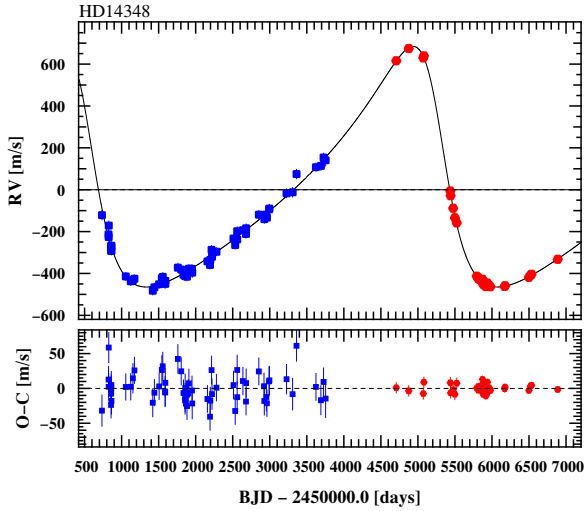
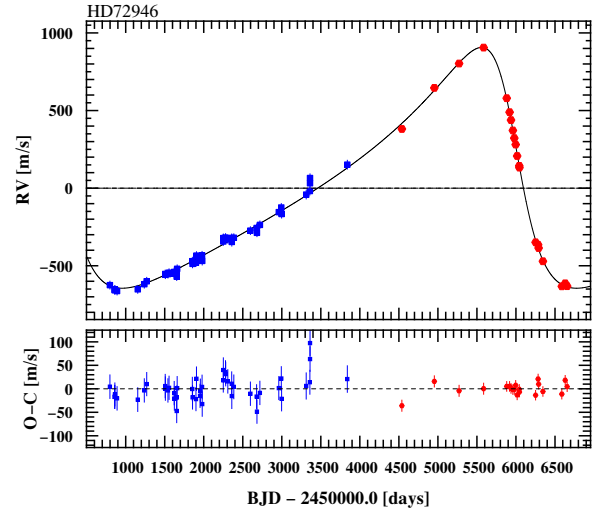**Fig. 4.** Radial velocity curve of HD 14348.

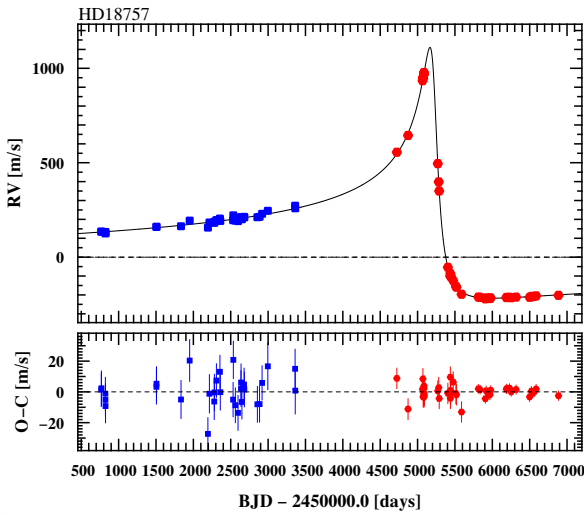**Fig. 6.** Radial velocity curve of HD 72946.

Fig. 5. Radial velocity curve of HD 18757.

4.3. HD 18757

HD 18757 is a bright $V = 6.64$ mag G4V star with low metallicity located at only 24.2 parsec from the Sun. HD 18757 is part of a multiple system with an M-dwarf component of $V = 12.5$ located at 12.7 arcsec (307 AU; Dommanget & Nys 2002) and a physically associated common proper motion companion with a separation of 262 arcsec (6340 AU) and a spectral type of M2V (Raghavan et al. 2010). The RV measurements listed in Table 7 are fitted by a 109-yr Keplerian orbit with a semi-amplitude $K = 666$ m s^{-1} and a high eccentricity $e = 0.94$. The spectral analysis together with the comparison with evolutionary models yields a stellar mass of $M_\star = 0.88\ M_\odot$ and a companion minimum mass of 35.2 $M_{\rm Jup}$. Although a small fraction (17%) of the orbital period is covered, the Keplerian fit is sufficiently well constrained because the orbit is highly eccentric and the RV extrema are covered. The instrumental offset between ELODIE and SOPHIE is adjusted to $-120^{+9.5}_{-8.0}$ m s^{-1}, which is marginally higher than the expected offset at -66 ± 23 m s^{-1}. Systematic errors of 1.4 m s^{-1} and 2.7 m s^{-1} were quadratically added to ELODIE and SOPHIE, respectively. The large distance of the companion and the vicinity of the target allows placing a quite

strong constraint on the mass upper limit derived from PUEO observations with $Mc \leq 0.13\ M_\odot$.

4.4. HD 72946

HD 72946 is a $V = 7.25$ mag G5 star with a mass of 0.96 $M_\odot$ located at 26.2 parsec from the Sun. HD 72946 (GJ 310.1B) has a physically associated common proper motion companion HD 72945 (GJ 310.1A) located at 10 arcsec (230 AU). This companion is a spectroscopic binary with a period of 14.3 days including an F8V primary of $mv = 5.99$ (Duquennoy & Mayor 1991). We checked that this bright component located at 10 arcsec cannot introduce contaminating light within the 3-arcsec fiber acceptance of SOPHIE. Even with a seeing as high as 6 arcsec, the contamination remains lower than 0.3% and therefore is negligible. HD 72946 is also part of a multiple stellar system with a $V = 10.7$ star at 93 arcsec and a $V = 12$ star at 117 arcsec (Dommanget & Nys 2002). The Keplerian fit to the RV measurements listed in Table 8 indicates a companion of minimum mass $Mc \sin i = 60.4\ M_{\rm Jup}$ in a 16-yr orbit, with an eccentricity $e = 0.495$. The instrumental offset between ELODIE and SOPHIE is adjusted to -113 ± 14 m s^{-1}, which fully agrees with the expected offset of -100 ± 23 m s^{-1}. Systematic errors of 22 m s^{-1} and 15 m s^{-1} were quadratically added to ELODIE and SOPHIE, respectively, which may be due to the fact that the star is slightly active ($\log R'_{\rm HK} = -4.74$). Although a non-significant drift was found from fixing the instrument offset, we note that the F8V companion at 230 AU may introduce a radial velocity change on HD 72946 of up to few m s^{-1} per year.

4.5. HD 209262

HD 209262 is a $V = 8.0$ G-type star located at 49.7 parsec from the Sun. HD 209262 is part of a double system (Dommanget & Nys 2002) with a component BD+044788B ($V = 9.8$) at 78.3 arcsec and possibly a third component ($V = 12.4$) at 22.4 arcsec. The RV measurements listed in Table 9 are fitted by a 15-yr Keplerian orbit with a semi-amplitude of 385 m s^{-1} and an eccentricity $e = 0.35$. The spectral analysis combined with the comparison with evolutionary models yields a stellar mass of $M_\star = 1.02\ M_\odot$ and a companion minimum mass of 32.3 $M_{\rm Jup}$. The instrumental offset between ELODIE and SOPHIE is adjusted to -165 ± 24 m s^{-1}, which is marginally

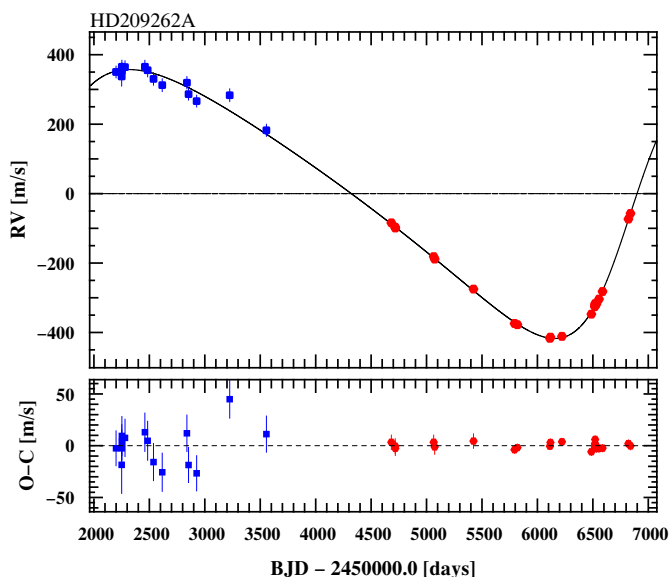**Fig. 7.** Radial velocity curve of HD 209262.

higher than the expected offset at -91 ± 23 m s^{-1}. Systematic errors of 14.3 m s^{-1} and 3.3 m s^{-1} were quadratically added to ELODIE and SOPHIE, respectively.

5. Discussion and conclusion

We have reported the detection of five new potential brown dwarf companions with minimum masses of between 32 and 83 $M_{\rm Jup}$ orbiting solar-type stars with periods longer than ten years. These detection were made thanks to ELODIE and SOPHIE radial velocity measurements that cover a time span of up to 16 yr. Our different diagnostics allowed excluding companions heavier than 0.4 $M_\odot$ and for HD 18757 heavier than 0.13 $M_\odot$. These candidates double the number of known BD companions with orbital periods longer than ten years, which include HD 4747, HD 74014, HD 211847, and HD 167665 (Sahlmann et al. 2011) that were detected in the CORALIE RV survey, and HIP 5158 (Lo Curto et al. 2010; Feroz et al. 2011) from the HARPS RV survey. This last one, HIP 5158b, should probably be considered a planetary candidate given its minimum mass of 15 ± 10 $M_{\rm Jup}$. This increasing number of long-period BD companions reinforces the observation that the number of BDs increases with orbital period, as pointed out by Ma & Ge (2014). All our BD candidates have an eccentricity higher than 0.45 except for the lightest one, HD 209262b, with $e = 0.35$. Three of our five targets are part of a multiple stellar system. All our targets, with a projected separation larger than 100 mas, and especially HD 18757 with 917 mas, will be good targets for high-contrast and high angular resolution imaging, interferometry, or speckle observations. Such targets are important to constrain the mass–luminosity relation of brown dwarfs for different ages and metallicity. Micro-arcsecond astrometry with the *Gaia* satellite (Mignard 2011) will permit deriving constraints on the orbital inclination and the true mass of these companions.

References

Allard, F., Hauschildt, P. H., Alexander, D. R., Tamanai, A., & Schweitzer, A. 2001, ApJ, 556, 357
Baraffe, I., Chabrier, G., Allard, F., & Hauschildt, P. H. 1998, A&A, 337, 403
Baraffe, I., Homeier, D., Allard, F., & Chabrier, G. 2015, A&A, 577, A42
Baranne, A., Queloz, D., Mayor, M., et al. 1996, A&AS, 119, 373
Boisse, I., Eggenberger, A., Santos, N. C., et al. 2010, A&A, 523, A88
Boisse, I., Bouchy, F., Hébrard, G., et al. 2011, A&A, 528, A4
Boisse, I., Pepe, F., Perrier, C., et al. 2012, A&A, 545, A55
Bouchy, F., Hébrard, G., Udry, S., et al. 2009, A&A, 505, 853
Bouchy, F., Díaz, R. F., Hébrard, G., et al. 2013, A&A, 549, A49
Bressan, A., Marigo, P., Girardi, L., et al. 2012, MNRAS, 427, 127
Burrows, A., Marley, M., Hubbard, W. B., et al. 1997, ApJ, 491, 856
Chabrier, G., & Baraffe, I. 2000, ARA&A, 38, 337
Collier Cameron, A., Wilson, D. M., West, R. G., et al. 2007, MNRAS, 380, 1230
Courcol, B., Bouchy, F., Pepe, F., et al. 2015, A&A, 581, A38
da Silva, L., Girardi, L., Pasquini, L., et al. 2006, A&A, 458, 609
Delfosse, X., Forveille, T., Beuzit, J.-L., et al. 1999, A&A, 344, 897
Díaz, R. F., Santerne, A., Sahlmann, J., et al. 2012, A&A, 538, A113
Díaz, R. F., Almenara, J. M., Santerne, A., et al. 2014, MNRAS, 441, 983
Dommanget, J., & Nys, O. 2002, VizieR Online Data Catalog: I/274
Doyon, R., Nadeau, D., Vallee, P., et al. 1998, in Infrared Astronomical Instrumentation, ed. A. M. Fowler, SPIE Conf. Ser., 3354, 760
Duquennoy, A., & Mayor, M. 1991, A&A, 248, 485
Feroz, F., Balan, S. T., & Hobson, M. P. 2011, MNRAS, 416, L104
Gregory, P. C. 2007, MNRAS, 374, 1321
Grether, D., & Lineweaver, C. H. 2006, ApJ, 640, 1051
Griffin, R. F. 2012, JApA, 33, 29
Griffin, R. F., Griffin, R. E. M., Gunn, J. E., & Zimmerman, B. A. 1988, AJ, 96, 172
Kolbl, R., Marcy, G. W., Isaacson, H., & Howard, A. W. 2015, AJ, 149, 18
Lo Curto, G., Mayor, M., Benz, W., et al. 2010, A&A, 512, A48
Ma, B., & Ge, J. 2014, MNRAS, 439, 2781
Mason, B. D., McAlister, H. A., Hartkopf, W. I., & Bagnuolo, Jr., W. G. 1993, AJ, 105, 220
Mayor, M., & Queloz, D. 1995, Nature, 378, 355
Mignard, F. 2011, Adv. Space Res., 47, 356
Mordasini, C., Alibert, Y., Benz, W., & Naef, D. 2009, A&A, 501, 1161
Naef, D., Mayor, M., Beuzit, J. L., et al. 2004, A&A, 414, 351
Nidever, D. L., Marcy, G. W., Butler, R. P., Fischer, D. A., & Vogt, S. S. 2002, ApJS, 141, 503
Patel, S. G., Vogt, S. S., Marcy, G. W., et al. 2007, ApJ, 665, 744
Patience, J., Ghez, A. M., Reid, I. N., Weinberger, A. J., & Matthews, K. 1998, AJ, 115, 1972
Perrier, C., Sivan, J.-P., Naef, D., et al. 2003, A&A, 410, 1039
Perruchot, S., Kohler, D., Bouchy, F., et al. 2008, in SPIE Conf. Ser., 7014
Raghavan, D., McAlister, H. A., Henry, T. J., et al. 2010, ApJS, 190, 1
Rigaut, F., Salmon, D., Arsenault, R., et al. 1998, PASP, 110, 152
Sahlmann, J., Ségransan, D., Queloz, D., et al. 2011, A&A, 525, A95
Santerne, A., Díaz, R. F., Almenara, J.-M., et al. 2015, MNRAS, 451, 2337
Santos, N. C., Israelian, G., & Mayor, M. 2004, A&A, 415, 1153
Santos, N. C., Sousa, S. G., Mortier, A., et al. 2013, A&A, 556, A150
Ségransan, D., Mayor, M., Udry, S., et al. 2011, A&A, 535, A54
Sousa, S. G., Santos, N. C., Mayor, M., et al. 2008, A&A, 487, 373
Spiegel, D. S., Burrows, A., & Milsom, J. A. 2011, ApJ, 727, 57
Torres, G., Andersen, J., & Giménez, A. 2010, A&ARv, 18, 67
Turner, N. H., ten Brummelaar, T. A., McAlister, H. A., et al. 2001, AJ, 121, 3254
van Leeuwen, F. 2007, A&A, 474, 653
Zechmeister, M., & Kürster, M. 2009, A&A, 496, 577
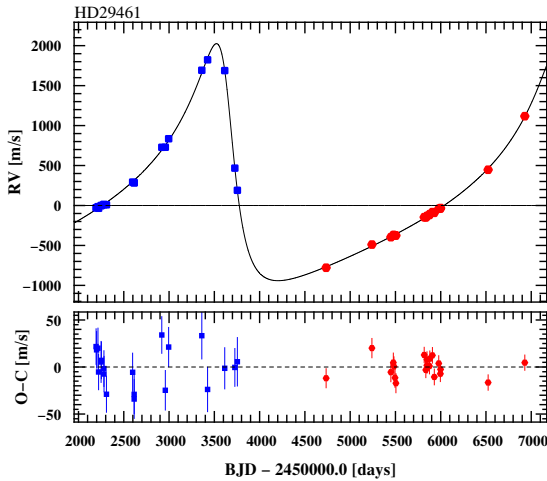
Appendix A: HD 29461

Fig. A.1. Radial velocity curve of HD 29461.

HD 29461 is a $V = 7.96$ mag G5-type star located at 46.5 parsec from our Sun. It was first identified as a spectroscopic binary in the Hyades field by Griffin et al. (1988) with a period of about ten years. Mason et al. (1993) and Patience et al. (1998) failed to resolve the system by speckle interferometry, indicating that the companion is very faint with a mass upper limit of 0.22 $M_\odot$. Patel et al. (2007) gave a preliminary orbit for HD 29461 from Keck observations that did not cover a complete cycle. The period they selected was 18 yr. More recently, Griffin (2012) published the orbital elements derived from 78 radial velocity measurements spanning 38 yr, from 1972 to 2009. The Keplerian fit yields a period $P = 3760 \pm 8$ days, a semi-amplitude $K = 1.36 \pm 0.04$ km s^{-1}, and an eccentricity $e = 0.594 \pm 0.019$.

For this target we obtained 20 ELODIE and 20 SOPHIE measurements in a time span of 13 yr. Our measurements, displayed in Fig. A.1, confirm and agree with the orbital parameters derived by Griffin (2012), except for our semi-amplitude ($K = 1.483 \pm 0.015$ km s^{-1}), which is 3σ higher. The instrumental offset between ELODIE and SOPHIE is fitted to -167 ± 16 m s^{-1}, which is marginally higher than the expected offset at -78 ± 23 m s^{-1}. This slightly higher offset can explain the larger semi-amplitude found. Systematic errors of 15 m s^{-1} and 8 m s^{-1} were quadratically added to ELODIE and SOPHIE,

respectively. The star is slightly active with $\log R'_{\rm HK} = -4.73$, which may explain the RV jitter observed in SOPHIE measurements. We derive a period $P = 3776 \pm 12$ days and an eccentric $e = 0.613 \pm 0.004$. The spectral analysis and the comparison with evolutionary models yields a stellar mass of $M_\star = 1.06 \pm 0.07$ $M_\odot$ and a companion minimum mass of 93.4 $M_{\rm Jup}$, which firmly excludes a brown-dwarf companion.

Appendix B: HD 175225

HD 175225 is a $V = 5.5$ mag G9 subgiant located at 26.1 parsec from our Sun. Turner et al. (2001) made a direct detection of a companion at 1.1 arcsec (28.7 AU) using the adaptive optics system at Mount Wilson Observatory. They estimated from the $V - I$ color that the companion corresponds to an M2 dwarf. Considering the separation, the orbital period is expected to be about 150 yr. For this target we obtained 38 CORAVEL, 38 ELODIE, and 16 SOPHIE measurements in a time span of 31.7 yr. Radial velocities, displayed in Fig. B.1, show a long-term trend with curvature. The Keplerian fit is no constraint, but indicates an orbital period longer than 45 yr and a companion heavier than 0.2 $M_\odot$, which is fully compatible with the direct imaging.
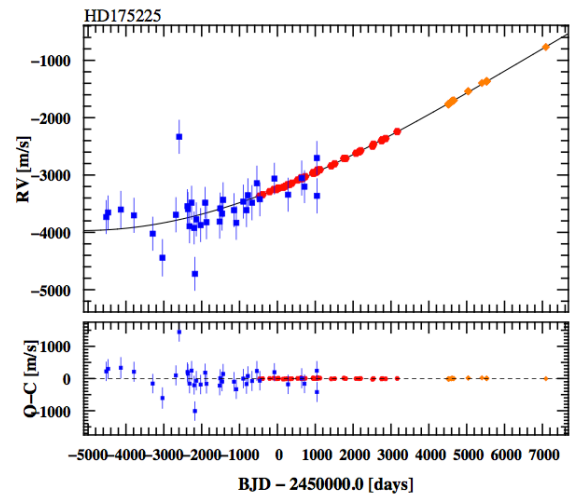

Fig. B.1. Radial velocity curve of HD 175225 obtained with CORAVEL (blue), ELODIE (red), and SOPHIE (orange)